Supporting Information for

Direct Conjugation with Zero Length Linker of Fullerene C_{70} to ZnO Quantum Dots for Multicolor Light-Emitting Diodes

Young Jae Park[1†], Jaeho Shim[1†], Kyu Seung Lee[1†], Won Ki Lee[1], Jun Yeon Hwang[1], Hyunbok Lee[2], Yeonjin Yi[3], Basavaraj Angadi[4], Won Kook Choi[5], and Dong Ick Son[1,6*]

*Corresponding author. E-mail: eastwing33@kist.re.kr

Table of Contents

†These authors contributed equally to this work.
*Corresponding author. E-mail: eastwing33@kist.re.kr (D. I. S.)

Materials and Methods

Synthesis of ZnO QDs

1.84 g of zinc acetate dihydrate [$Zn(CH_3COO)_2 \cdot 2H_2O$] was dispersed in 240 ml of N,N-Dimethylformamide (DMF, $HCON(CH_3)_2$). The solution was maintained at 140 °C for 5 h, while stirring continuously. The ZnO QDs solution was purified with ethanol about 10 times by centrifugation and decantation, followed by washing with distilled water in the same way. The final ZnO QD powder was obtained after drying in an oven at 60 °C for 24 hr. The average size of ZnO QDs can be tailored under well-controlled concentration of precursor (zinc acetate dehydrate).

Fullerene C_{70} (C_{60}) functionalization with oxygen-containing groups.

The mixture of HNO_3 (18 mL, 17 M) and H_2SO_4 (54 mL, 18 M) in ratio of 1:3 was prepared and used for dissolving C_{70} (C_{60}) powder (5 g, 99%, Sigma Aldrich, USA) with ultrasonication at 45 °C for 2 h. The solution (72 mL) was placed in a cleaned glass bottle and maintained at room temperature for 4 days. The color of dispersion gradually became dark brown, indicating the formation of functional groups on the C_{70} (C_{60}). The dispersion was then washed several times with distilled water by centrifugation and decantation. The resulting functionalized C_{70} (C_{60}) precipitates were allowed to dry at 60 °C for 24 h. The final oxidized fullerene C_{70} (C_{60}) powders were obtained with a heavy brown appearance.

Synthesis of ZnO-C_{70} (ZnO-C_{60}) QDs.

The functionalized C_{70} (C_{60}) powder (40 mg) was dissolved in 40 ml of DMF with ultrasonication for 10 minutes. 1.84 g of Zinc acetate dihydrate [$Zn(CH_3COO)_2 \cdot 2H_2O$] was dispersed in 200 ml of DMF. The functionalized C_{70} (C_{60}) solution was then added and maintained at 140 ^oC for 5 h, while stirring continuously. The ZnO-C_{70} (ZnO-C_{60}) quantum-dot

solution was then purified with ethanol several times by centrifugation and decantation, followed by washing with distilled water in the same way. The final ZnO-C_{70} (ZnO-C_{60}) quantum-dot powder was obtained after drying in an oven at 60^{o}C for 24 hr.

Characterization of ZnO-C_{70} QDs.

The ZnO-C_{70} QDs were characterized through X-ray diffraction (XRD), high angle annular dark field (HAADF) and transmission electron microscopy (TEM). To closely examine the ZnO-C_{70} QDs, HR-TEM studies were performed on an FEI TITAN G2 equipped with an image Cs corrector and a monochromator at an acceleration voltage of 80 kV. This is to optimize the ghost effect at the spherical edge image due to the spherical aberration and to avoid knock-on damage of carbon nanostructure (fig. S4). TEM specimens were prepared under air condition using conventional drop and dry methods for ZnO-C_{70} QD powders after dispersed in ethanol. The image is calculated by extracting information from the diffraction pattern of the Fast-Fourier transform (FFT) image in Fig. 2d and then the inverse of the selectively obtained FFT image.

The XRD patterns were obtained by a Panalytical Empyrean X-ray Diffractometer using Cu Kα radiation. The PL emission was spectrally resolved using collection optics and a monochromator (SP-2150i, Acton).

X-ray photoemission spectroscopy (XPS) measurements were conducted with a ULVAC PHI5000 VERSA PROBE system. UPS spectra were collected with a PHI 5700 spectrometer and He Iα ($h\nu$ = 21.22 eV) ultraviolet light source. Time resolved photoluminescence (TRPL) was measured at room temperature with a laser excitation wavelength of 352 nm. In addition, the ZnO-C_{60} QDs were also characterized and presented in Supplementary Sections 2 and 8.

Hybrid Integrated Vacuum Analyzer System (fig. S7) was employed for analyzing of ZnO-C_{70} QDs to analyze structural properties and electronic structures of the materials, which

facilitates the SEM, Raman, and AFM (SKPM) measurements simultaneously inside the vacuum chamber without air exposure, resulting in trustworthy data with correlated nanometer scale analysis from the exact same position. We used a combined SEM-AFM-Raman for measuring work function of ZnO, ZnO-C_{60} and ZnO-C_{70} QDs. The combined SEM-AFM has a number of advantages in comparison to the two systems as stand-alone. The combination of SEM and AFM/Raman offers an exact positioning of the AFM tip/laser. The AFM measures precise information about topography, electrical and mechanical properties of the surface. The combined SEM-SPM system is based on the integration of a vacuum compatible SPM into the SEM systems. This design enables alignment the electron beam and the SPM tip with much higher accuracy because the beam and tip are moved without interference. Consequently, better performance in terms of resolution and frame rate can be achieved by this setup. The alignment of the laser path and the exchange of the cantilever and the sample can be performed without breaking the vacuum. The positioning of the SPM tip to the area of interest in respect to the SEM can be realized by remote control.

UPS measurement was carried out to clarify the electronic structures of ZnO QDs and ZnO-C_{70}. The Φ of ZnO, F-C_{70}, and ZnO-C_{70} were estimated by the difference between the energy of He Iα ($h\nu = 21.22$ eV) ultraviolet light source and the energy of the secondary electron cutoff (SEC).

DFT calculations.

Theoretical modeling was performed using a Becke's three parameters exchange and Lee-Yang-Parr correlation (B3LYP) hybrid functional and 6-31G(d) basis set implemented in the Gaussian 09 package. The geometries of three different functionalized (epoxy, hydroxy, and carboxy bonds) C_{70} molecules were fully relaxed and optimized structures were checked by vibrational frequency analysis. To determine the most probable structure with the lowest

total energy, 4 or 5 different positions of the functional group were attempted for each functionalized C_{70} and their total energies were compared after geometry relaxation.

LEDs utilizing the ZnO-C_{70} QDs.

The ZnO-C_{70} LED device with multilayered structure was fabricated using spin-coating method (fig S10). The ZnO-C_{70} QD solution was used for the emission layer. The fabrication process flow started with cleaning of the transparent patterned indium tin oxide (ITO) coated glass (ITO/glass) substrate by ultrasonicating sequentially in acetone, ethanol, isopropyl alcohol, and de-ionized water for 10 min, respectively. It is then dried with nitrogen gas blow, followed by the ultraviolet/ozone (UVO) treatment for 15 min in a chamber. The PEDOT:PSS polymer in isopropyl alcohol (2.39 wt%) solution, the poly(N,N′ -bis(4-butylphenyl)-N,N′ -bis(phenyl)benzidine) (poly-TPD) polymer in chlorobenzene (1.5 wt%) solution, the ZnO-C_{70} QD powder in ethanol solution (3.07 wt%), and Cs_2CO_3 in 2-ethoxyethanol solution (0.01 wt%) was spin-coated in sequence as a hole injection layer (HIL), a hole transport layer (HTL), an active layer of the LEDs, and an electron injection layer (EIL) and hole blocking layer (HBL), respectively. The annealing processes were performed to remove the solvent after each layer at 100, 120, 110, and 90 °C, for 30, 20, 20, and 10 min, respectively. Finally, 150 nm-thick aluminum was deposited as a top electrode by thermal evaporation. The effective area of the LEDs was 2 mm × 2 mm. J-V measurement for the fabricated LEDs was conducted with a programmable electrometer with built-in current and voltage measurement units (model 236, Keithley). Electroluminescence was measured at room temperature using a Spectra Scan PR-730 spectroradiometer.

Supplementary Text

TEM measurement

The TEM images of ZnO-C_{60} and ZnO-C_{70} QDs (figs. S2 and S3) show that the ZnO core QDs are covered by fullerene C_{60} or fullerene C_{70} molecules. Figure S4 shows that the fullerene C_{70} structures are rapidly collapsed by beam damage at an acceleration voltage of 300 kV. The spherical parts which are considered as fullerene C_{70} molecules are not observed.

Hybrid integrated vacuum analyzer system: SEM-AFM/Raman measurement.

An SKPM mapping provides the electrostatic forces between the AFM tip and the surface of the specimen with resolution in the nanometer range. The electrostatic force is zero when the contact potential difference (V_{CPD}) is compensated by applying a dc voltage to the tip that is equivalent to the V_{CPD} measured in SKPM. The V_{CPD} can be converted to the Φ of the specimen by calibrating the Φ of the AFM tip. Highly oriented pyrolytic graphite (HOPG) is used as a calibration standard for the Φ measurements since it generally does not form interface dipoles with typical ambient contaminants that can be found on the surface. The outstanding advantage of HOPG enables its Φ to be quite stable at around 4.6 eV. Hence, Φ of the AFM tip was calibrated by comparing it with that of HOPG.

Figure S8 and S9 show 5 × 5 μm^2 AFM topographic image, (scanning Kelvin probe microscopy) SKPM map, and line profile corresponding to the white line in SKPM maps for the highly oriented pyrolytic graphite (HOPG), functionalized C_{60} (F-C_{60}), and ZnO-C_{60} QDs. The SKPM maps were also measured at 5 × 5 μm^2 areas for all samples. Figure S7 c shows that the average surface potential of the HOPG was estimated to be -0.24 eV, resulting in the workfunction of the AFM tip of 4.36 eV. Figure S8 c and f presents that the workfunctions of F-C_{60} and ZnO-C_{60} were calculated to be

3.99 eV and 4.16 eV, respectively. These results are in good agreement with the experimental results of F-C_{70} and ZnO-C_{70}.

UPS measurement

Most ZnO nanoparticles are inclined towards a nonpolar surface. However, the Φ of ZnO QDs used in this study showed lower value of 3.86 eV than that of nonpolar surface of ZnO, which is similar to that of ZnO synthesized by solution method. The ionization energy of ZnO QDs is calculated to be 7.08 eV, which is close to the value of ZnO synthesized via a sol-gel method. As shown in Fig. 1d and 1e, the volume ratio of ZnO/C_{70} is very low due to the tiny size of the fullerene C_{70} attached to the ZnO QDs, which causes limited changes in the electronic structure, resulting in similar density of state to ZnO QDs.

Profiling of ZnO-C_{70} QD.

HR-HAADF (high resolution high angle annular dark field) combined with energy-dispersive X-ray spectroscopy (EDS) data scanned over a single particle demonstrates that the fullerene C_{70} is wrapped around ZnO QDs. The size of ZnO-C_{70} QD was measured to be around 16 nm, which is in good agreement with the size calculated from XRD and the EDS line profiles in fig. S5 (b). Figure S5 (b) represents drift corrected spectrum profile scanning EDS of C K line, O K line, and Zn L line of a ZnO-C_{70} QD, respectively. The intensity of carbon decreases down to 16 nm, then maintains similar value up to around 32 nm and then begins to increase again after 32 nm. Similarly, the intensities of Zn and O increase up to 16 nm and keep at similar mass level and then decrease after the position of 32 nm. These results suggest that the ZnO QD is well-covered with fullerene C_{70} molecules uniformly.

Nanoparticle diameter calculation by Debye-Scherrer Formula

The diameter of ZnO-C_{70} QDs was calculated using Scherrer equation which can be written as:

$$d = \frac{K\lambda}{\beta cos\theta}$$

where K is Scherrer's constant, typical value of 0.89 was used in this study, λ is the wavelength of X-rays, θ is the Bragg diffraction angle, and β is the full width and half maximum of the diffraction peak corresponding to <101> plane. XRD curves were recorded with CuK_α (λ=1.540598Å) radiation.

Time-resolved photoluminescence of ZnO-C_{60} QD and ZnO-C_{70} QD.

Time-resolved photoluminescence (TRPL) measurements of ZnO-C_{60} and ZnO-C_{70} were carried out with a laser (λ_{ex} = 352 nm) at room temperature to elucidate the charge transfer between the ZnO QDs and ZnO-C_{60} (ZnO-C_{70}). The lifetime (τ_1, τ_2) and average lifetime ($f_1\tau_1$+ $f_2\tau_2$) of each sample were estimated by fitting the PL decay curves using an exponential function, where f_1 and f_2 are the fractional intensities, τ_1 and τ_2 are the lifetimes, and χ^2 is the reduced chi-squared value. Table S5 and S6 contain detail information on the TRPL data.

Supplementary Figures

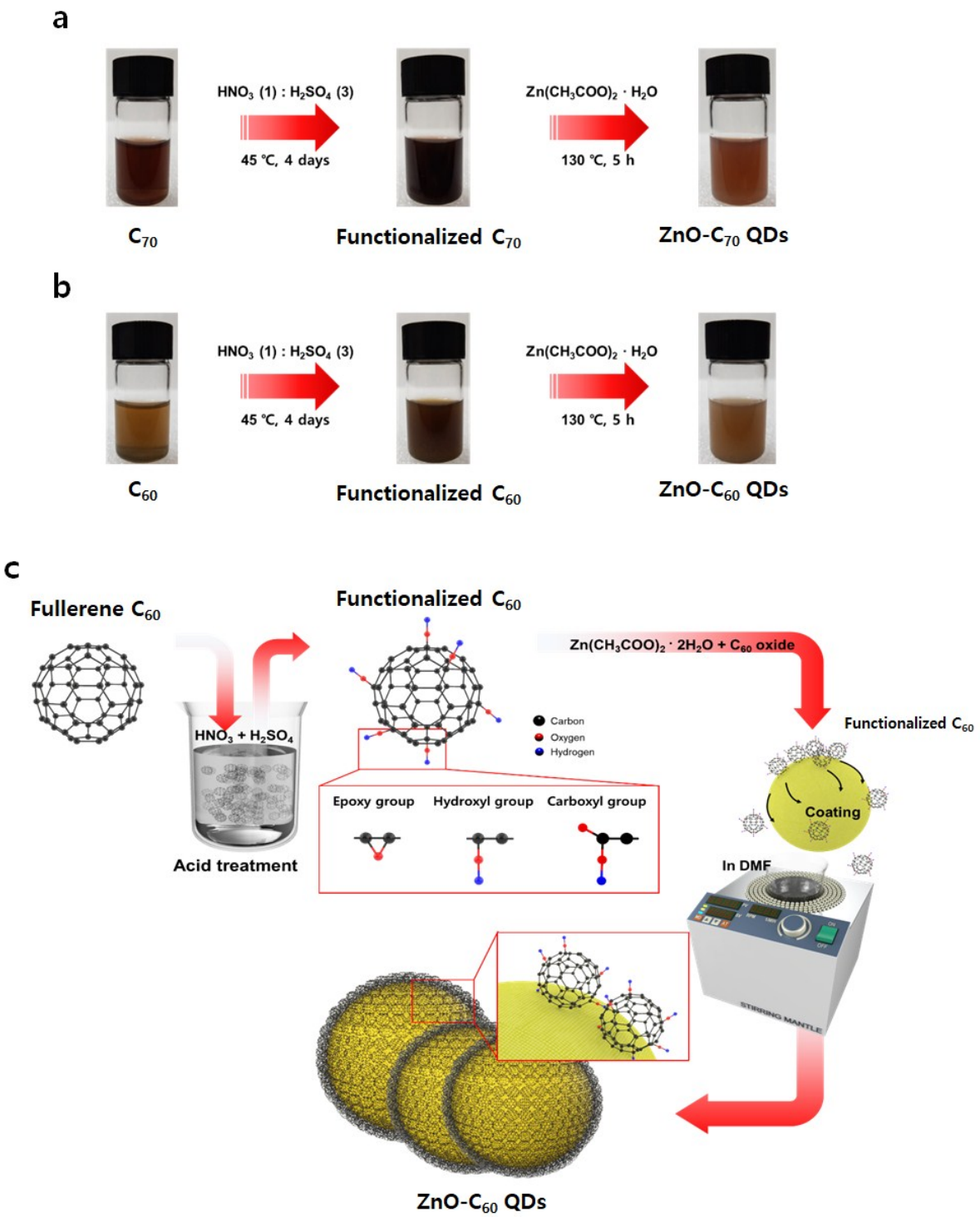

Figure S1. Chemical synthesis processes of ZnO QDs-functionalized fullerene (a) C_{70} and (b) C_{60}. (c) Schematic diagram of the synthesis process of the ZnO-C_{60}.

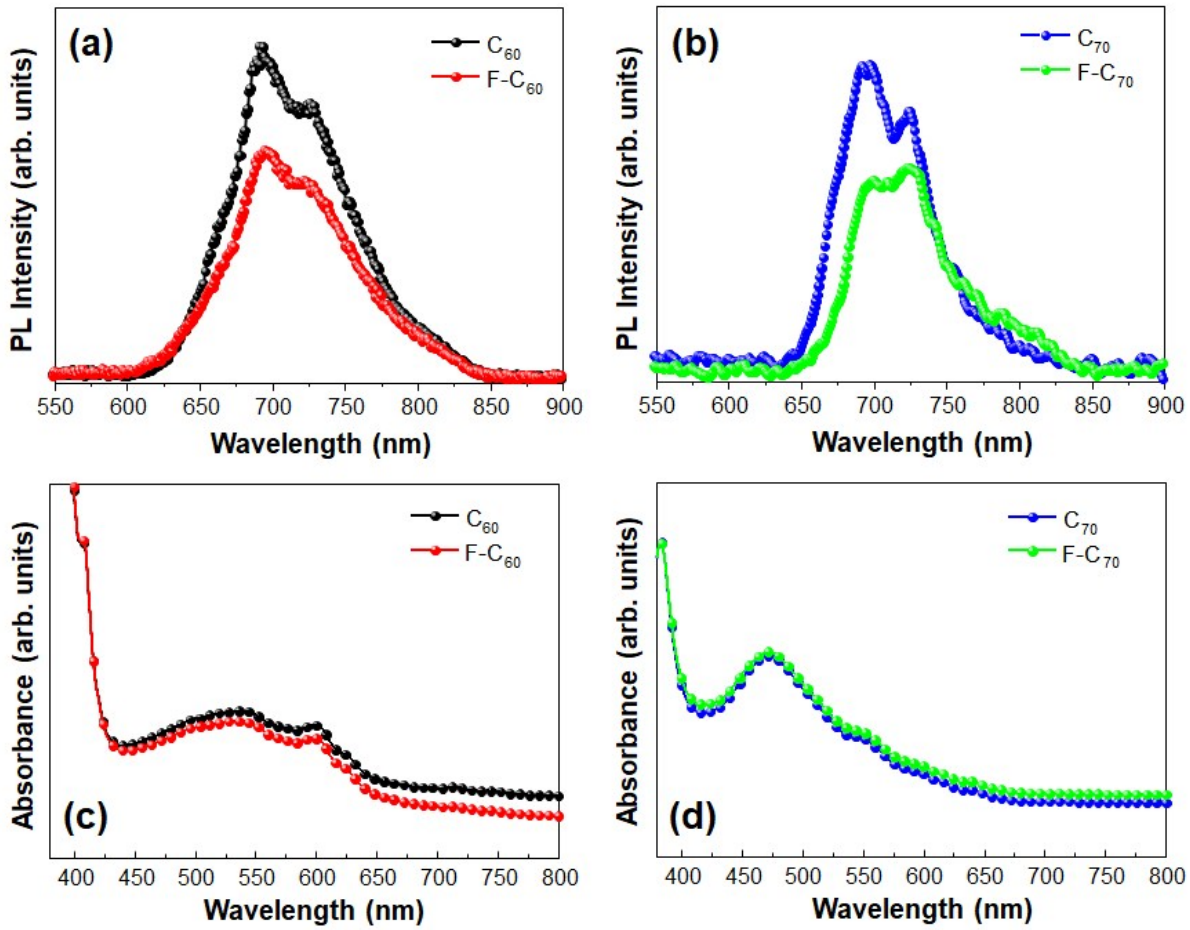

Figure S2. Photoluminescence spectra of (a) C_{60} and F-C_{60}, and (b) C_{70} and F-C_{70}. Absorbance spectra of (c) C_{60} and F-C_{60}, and (d) C_{70} and F-C_{70}.

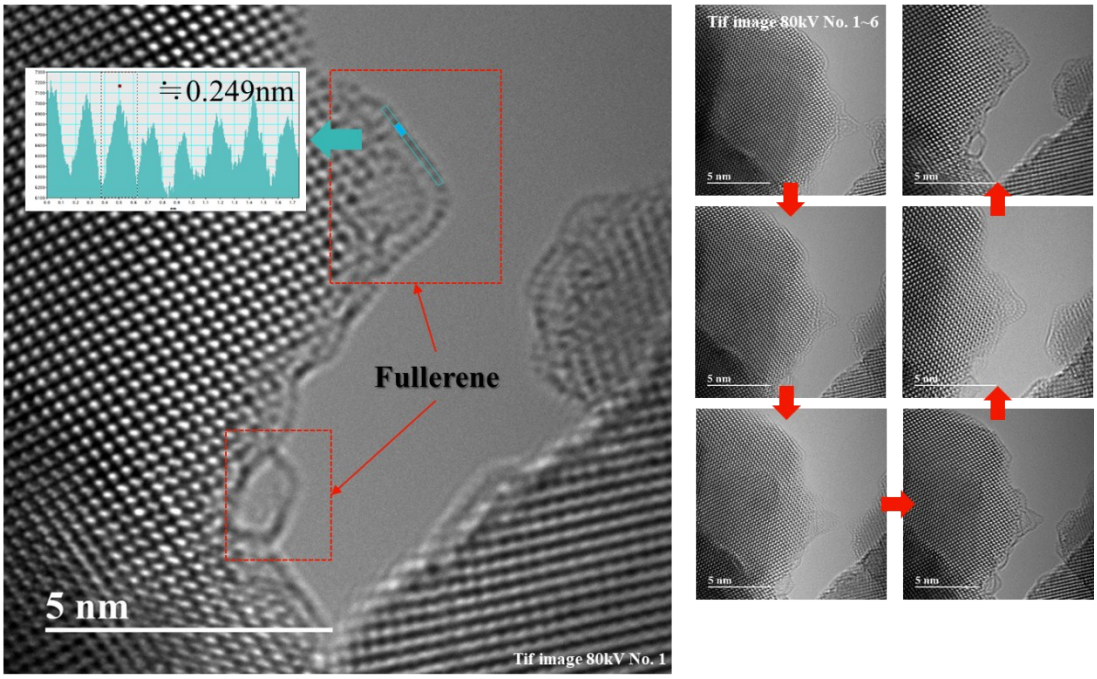

Figure S3. TEM images of the ZnO-C_{60} with various focal lengths of electron beam at an acceleration voltage of 80 kV.

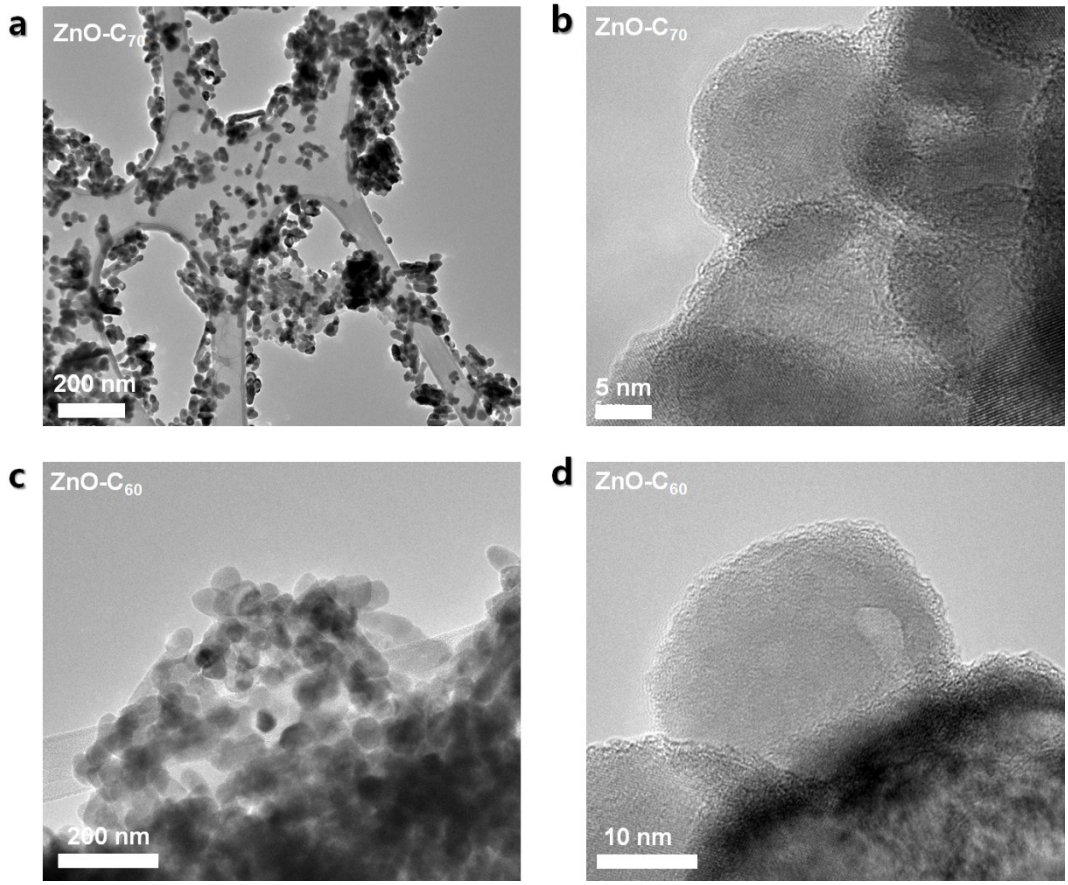

Figure S4. TEM images of (a, b) the ZnO-C_{70} and (c, d) the ZnO-C_{60}.

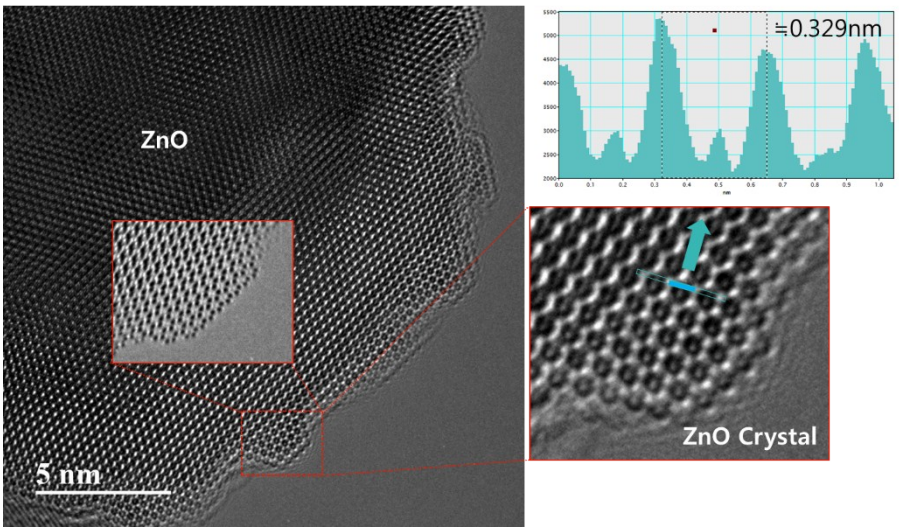

Figure S5. TEM images of the ZnO-C_{70} at an acceleration voltage of 300 kV

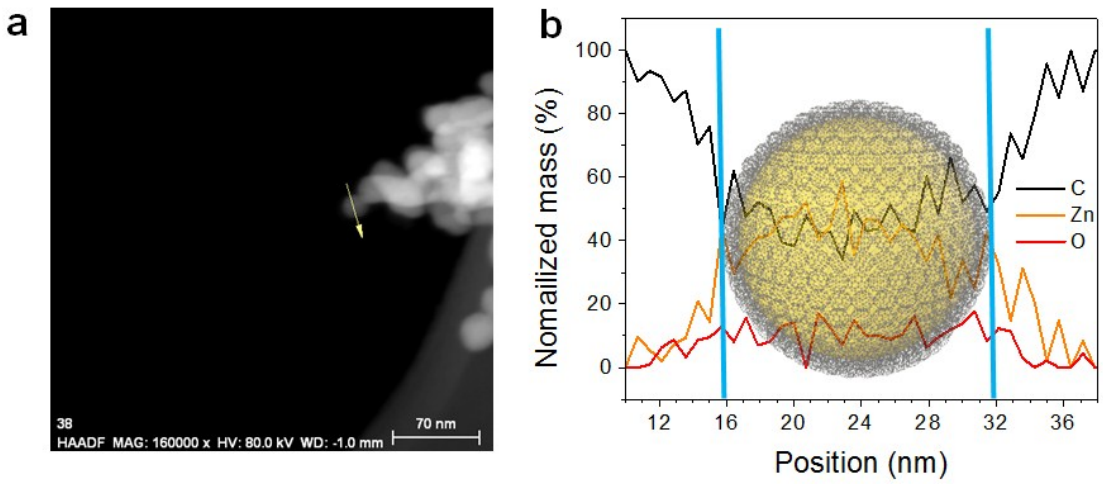

Figure S6. (a) HAADF image of ZnO-C_{70} QD, (b) EDS data along the yellow arrow.

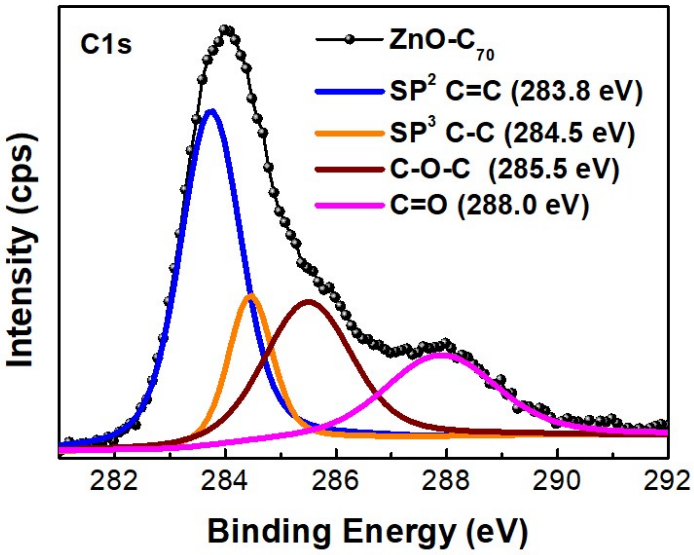

Figure S7. XPS spectra of ZnO-C_{70} with deconvoluted peaks.

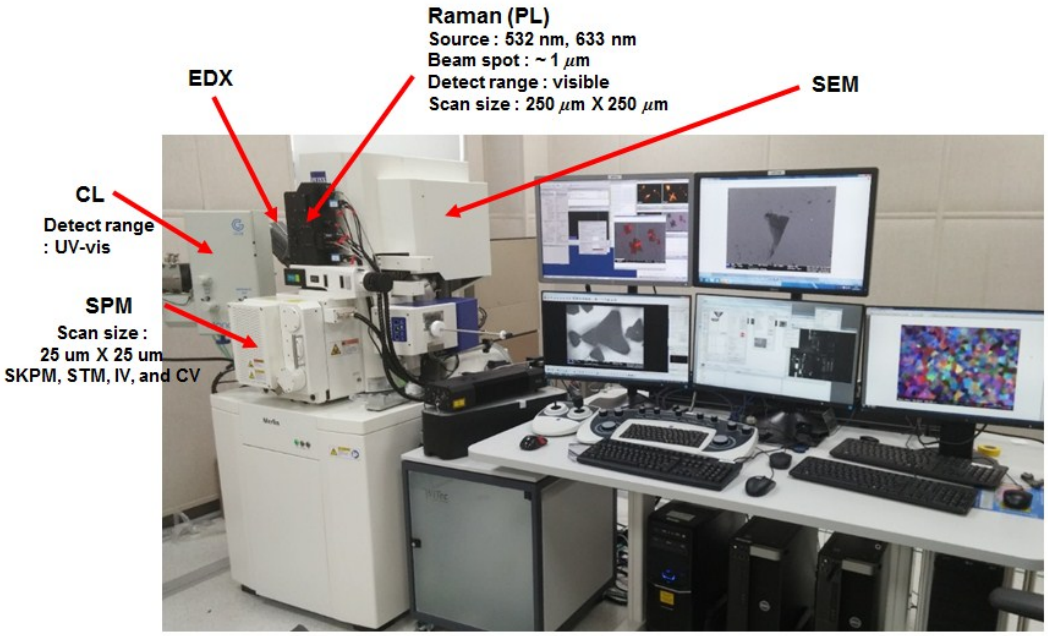

Figure S8. Image of Hybrid integrated vacuum analyzer system.

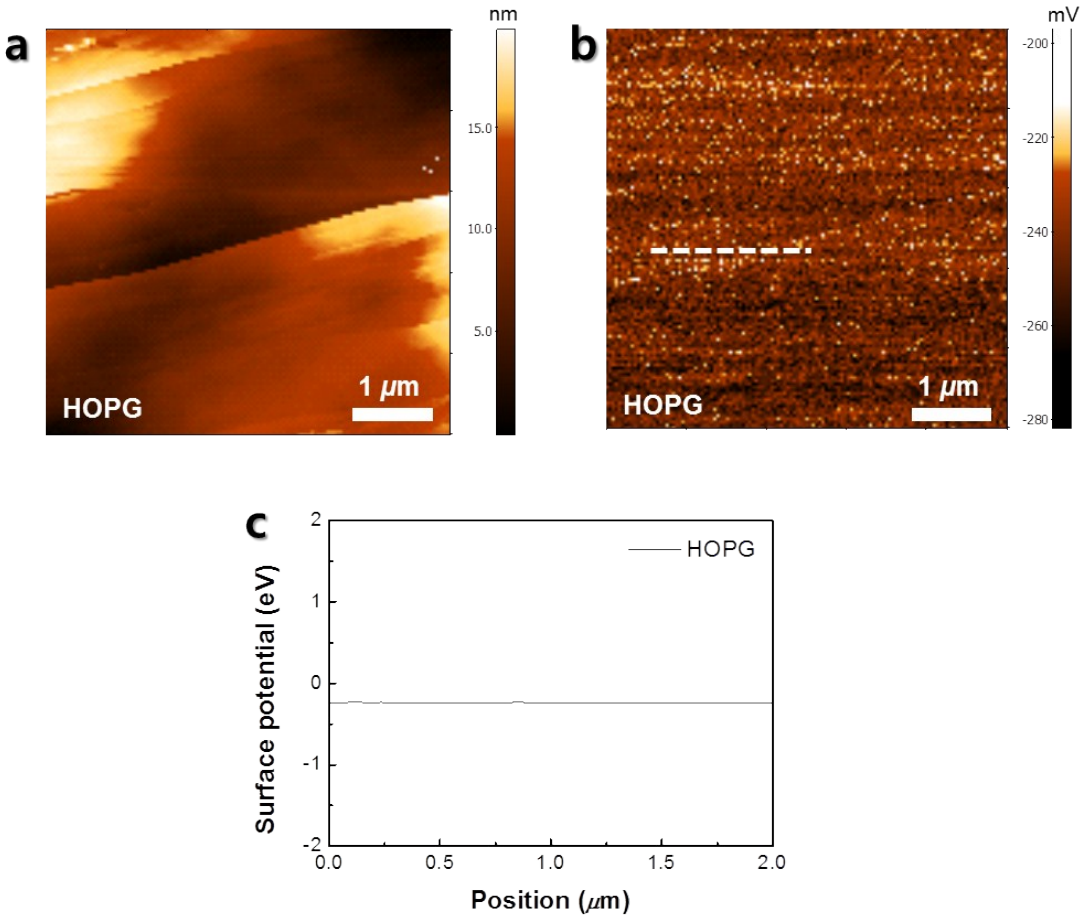

Figure S9. (a) 5 × 5 μm^2 AFM topography maps of HOPG. (b) SKPM maps of HOPG. (c) line profile corresponding to the white lines in Fig. S7.

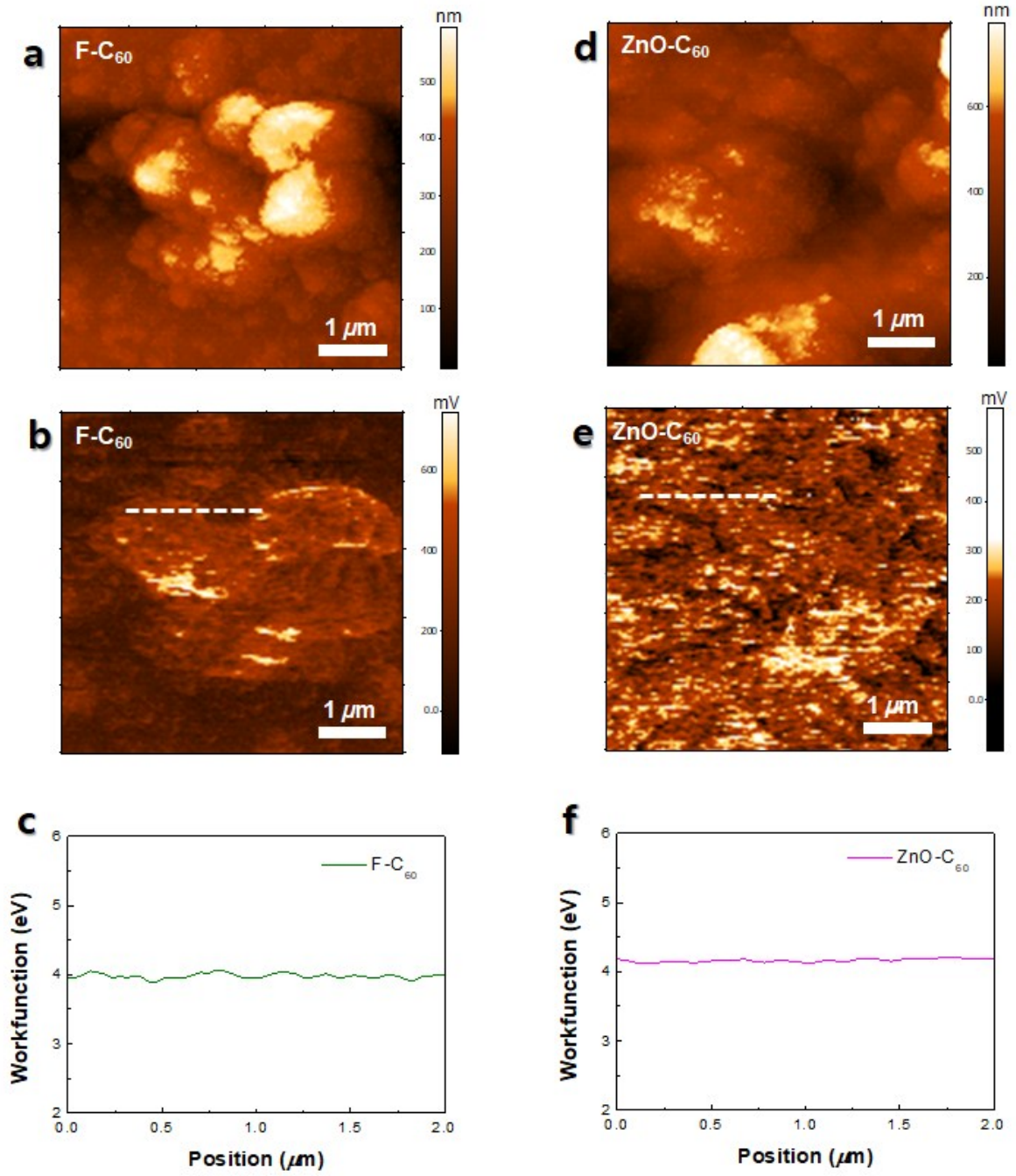

Figure S10. 5 × 5 μm^2 AFM topography maps of (a) F-C_{60} and (d) ZnO-C_{60}. SKPM maps of (b) F-C_{60} and (e) ZnO-C_{60}. Line profiles of (c) F-C_{60} and (f) ZnO-C_{60} corresponding to the white lines in Figs. S7 b and e, respectively.

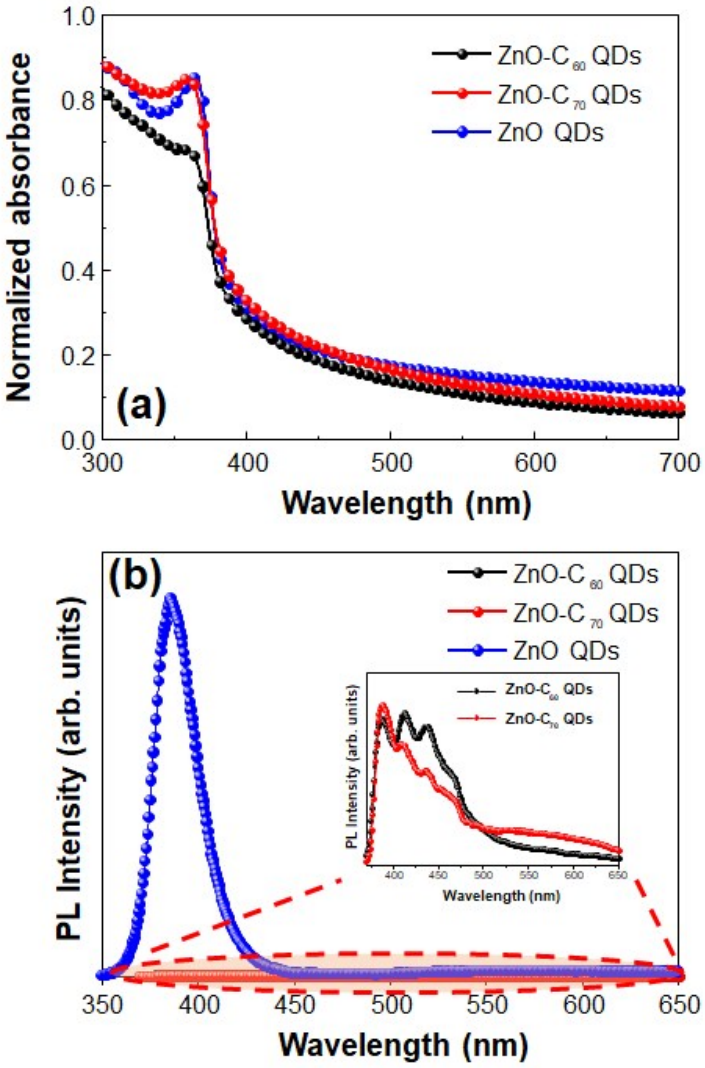

Figure S11. (a) Absorbance and (b) photoluminescence spectra of the ZnO-C_{60}, ZnO-C_{70}, and ZnO QDs.

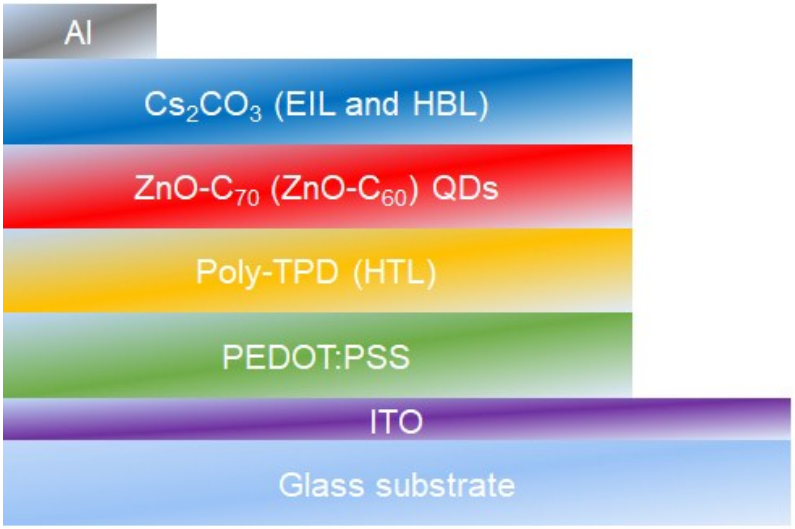

Figure S12. Schematic illustration of ZnO-C_{70} (ZnO-C_{60}) LEDs structures.

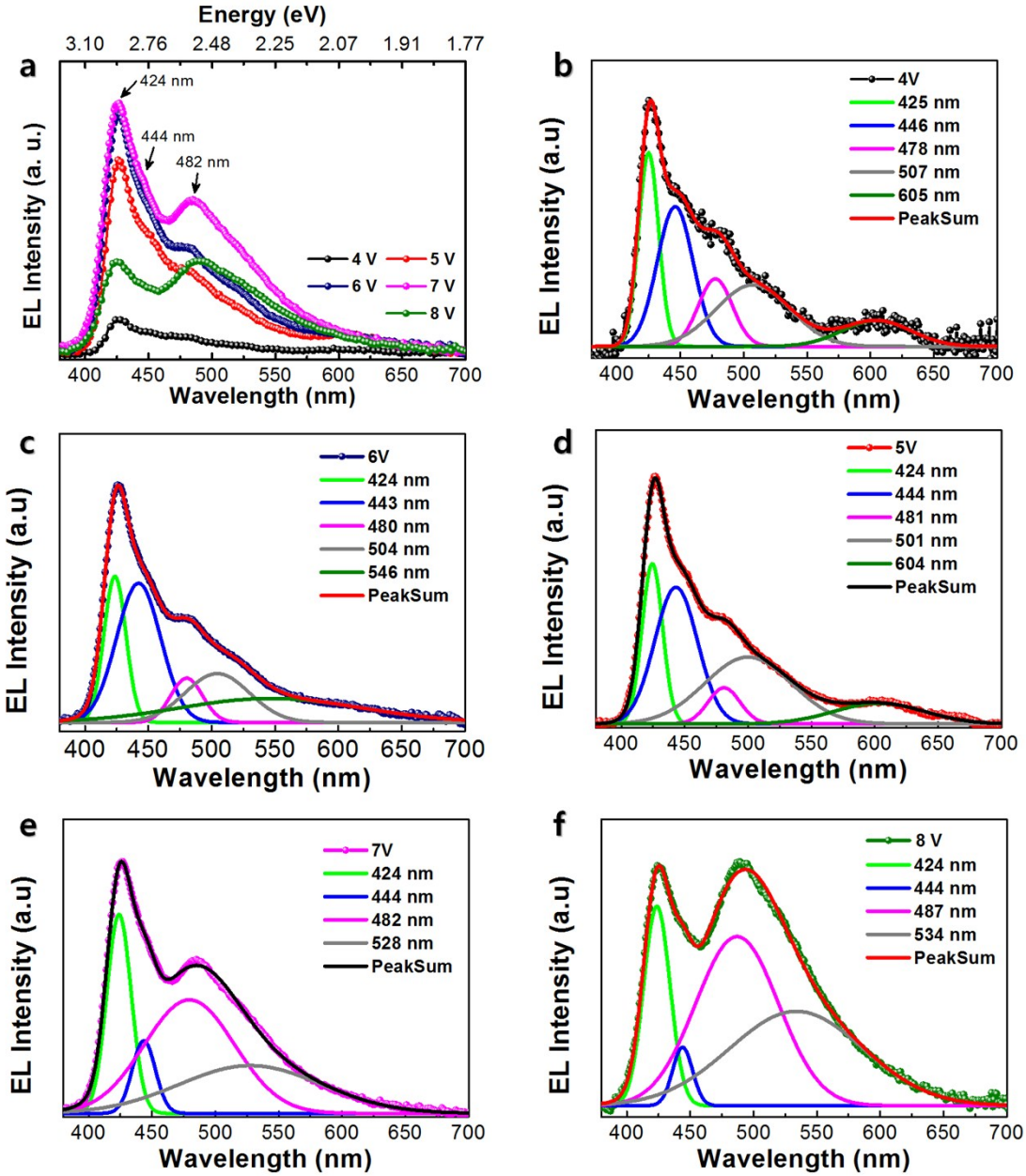

Figure S13. (a) Electroluminescence spectra of the ZnO-C_{70} LED with various applied voltages from 4 to 8 V. **(**b)-(f) Peak analysis for electroluminescence of ZnO-C_{70} LEDs at an applied bias of (b) 4V, (c) 5V, (d) 6V, (e) 7V, and (f) 8V. The electroluminescence spectra apparently show three distinct peaks wavelengths at around 424 nm (2.92 eV), 444 nm (2.79 eV), and 482 nm (2.57 eV), respectively, corresponding to 408 nm (3.04 eV), 436 nm (2.84 eV), and 460 nm (2.70 eV) observed from photoluminescence spectra.

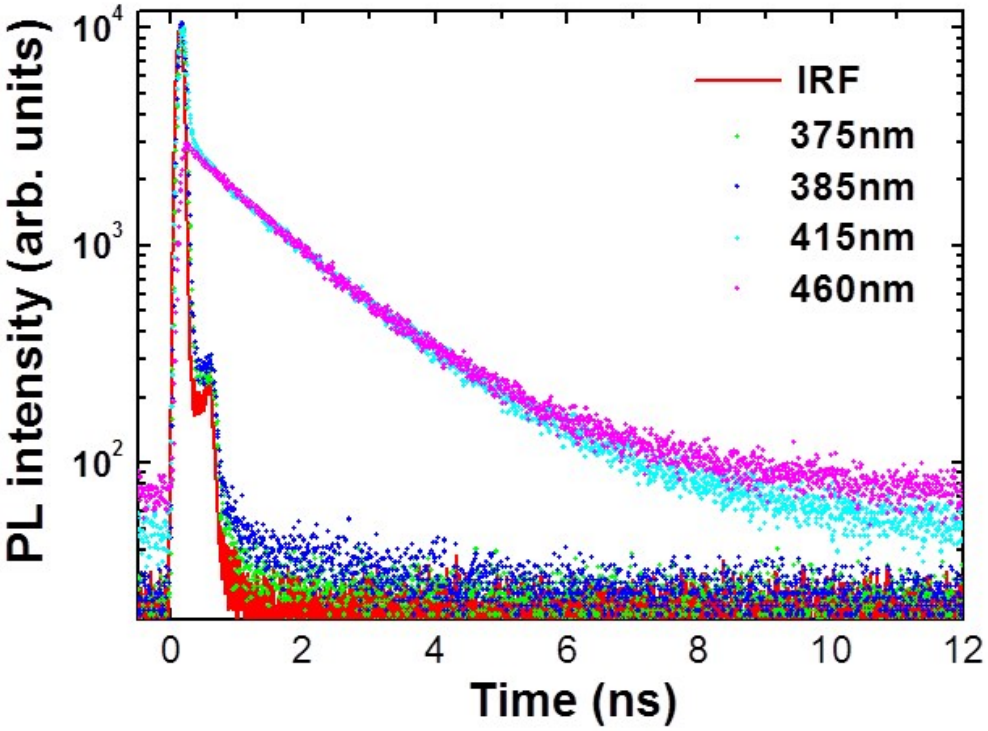

Figure S14. TRPL decay curves of ZnO-C_{60} QDs.

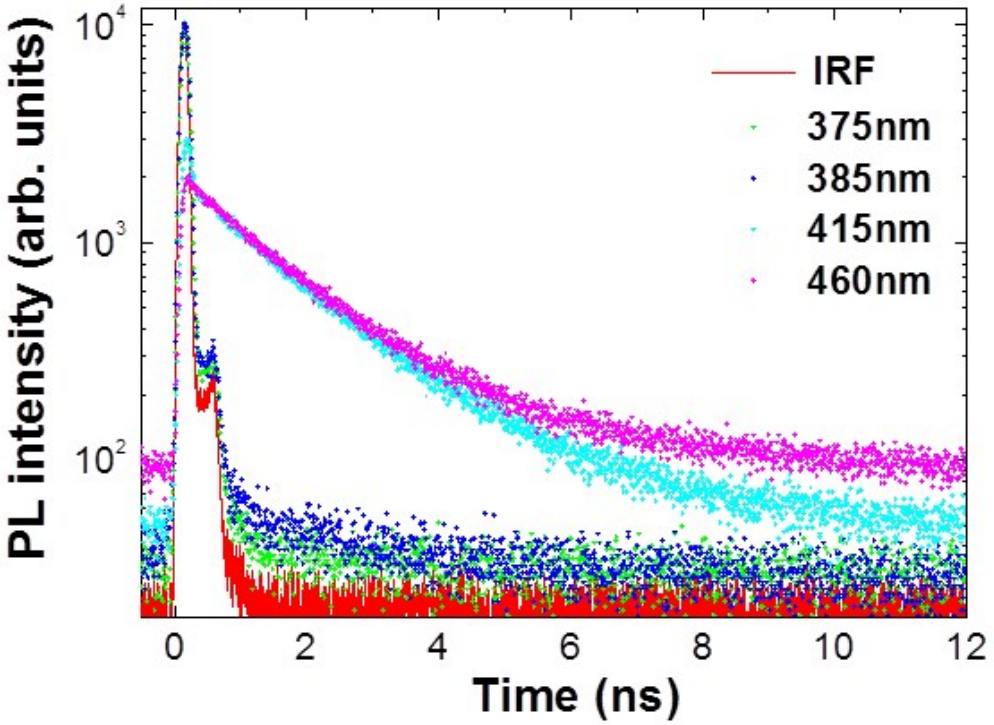

Figure S15. TRPL decay curves of ZnO-C_{70} QDs.

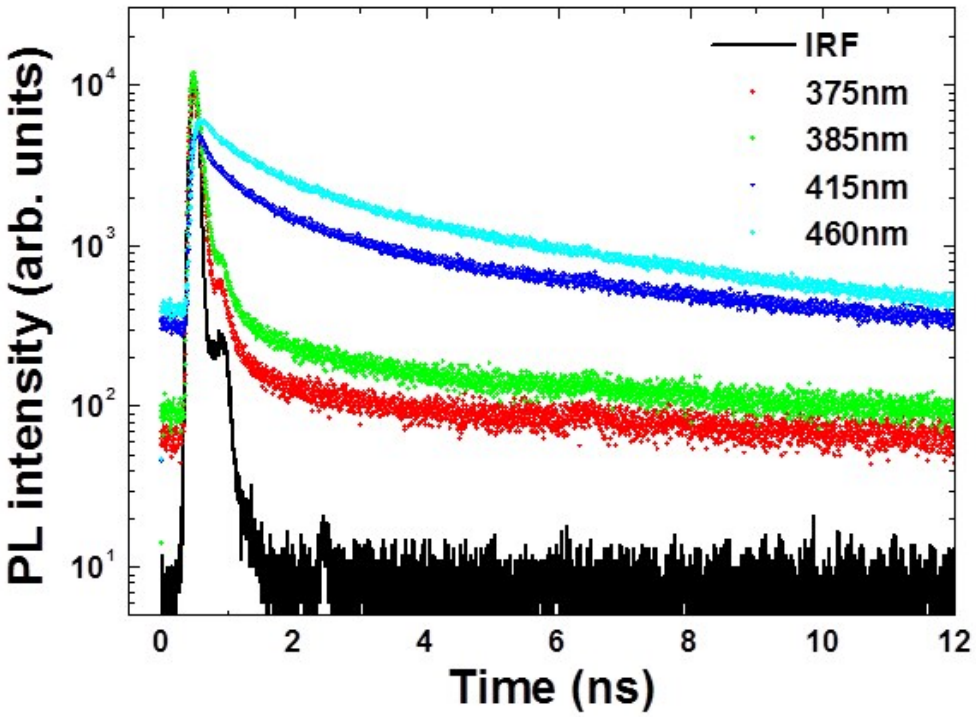

Figure S16. TRPL decay curves of ZnO QDs.

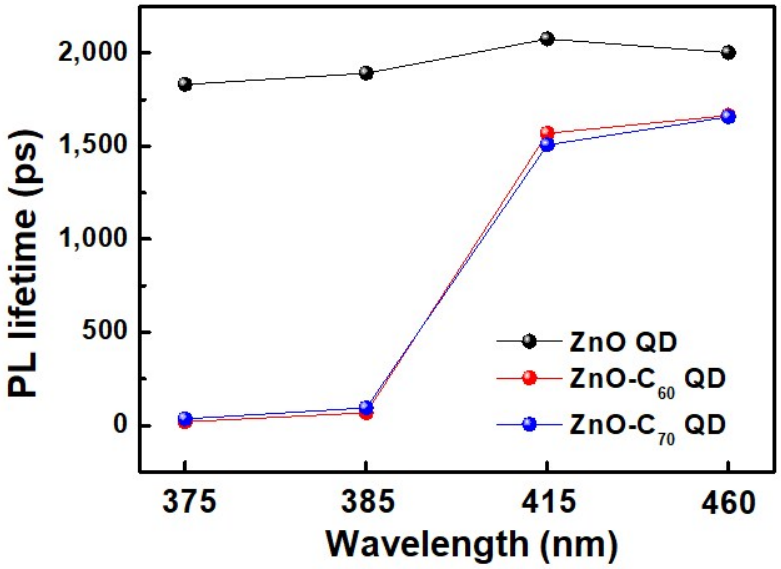

Figure S17. PL lifetimes of ZnO, ZnO-C_{60}, and ZnO-C_{70} QD.

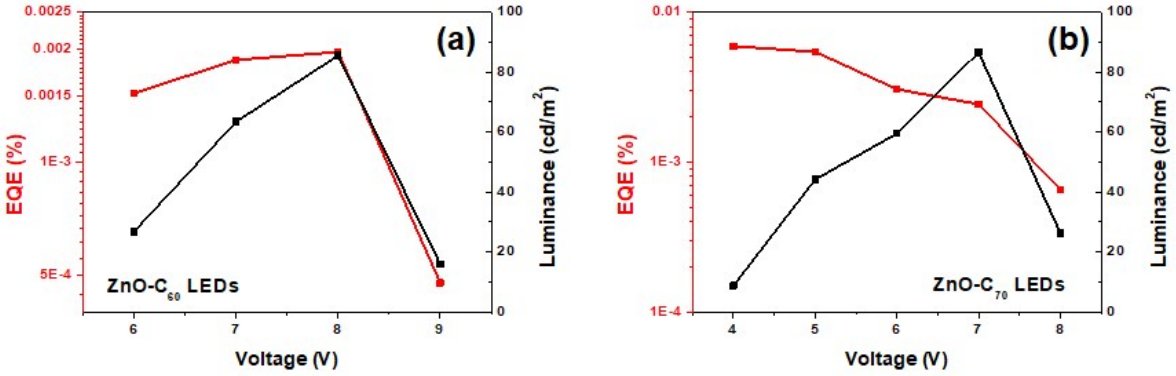

Figure S18. EQE and luminance of ZnO-C_{60}, and ZnO-C_{70} LEDs.

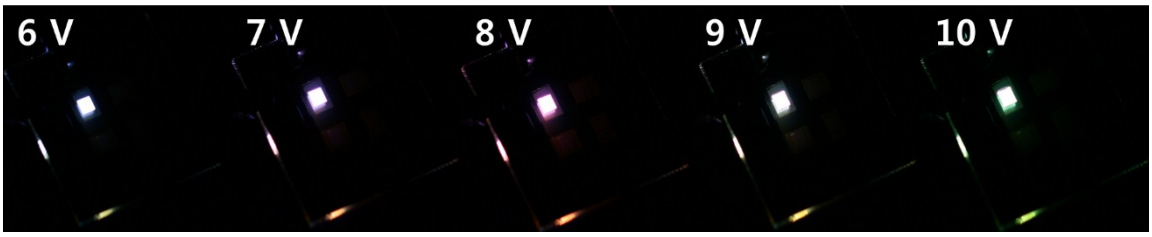

Figure S19. Photographs of ZnO-C_{60} LEDs for applied voltages of 6, 7, 8, 9, and 10 V, respectively.

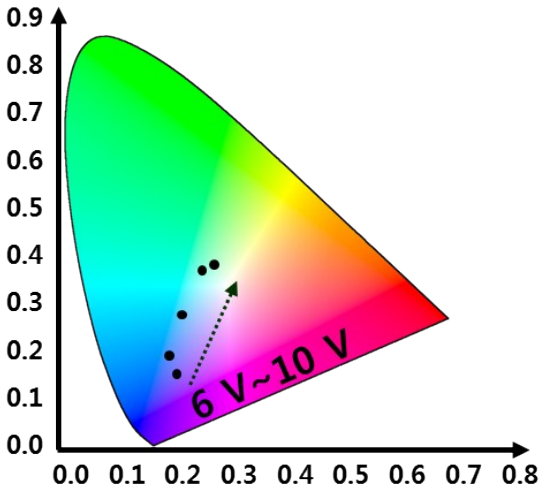

Figure S20. Change in color coordinate on a CIE (x,y) chromaticity diagram of ZnO-C_{60} LEDs.

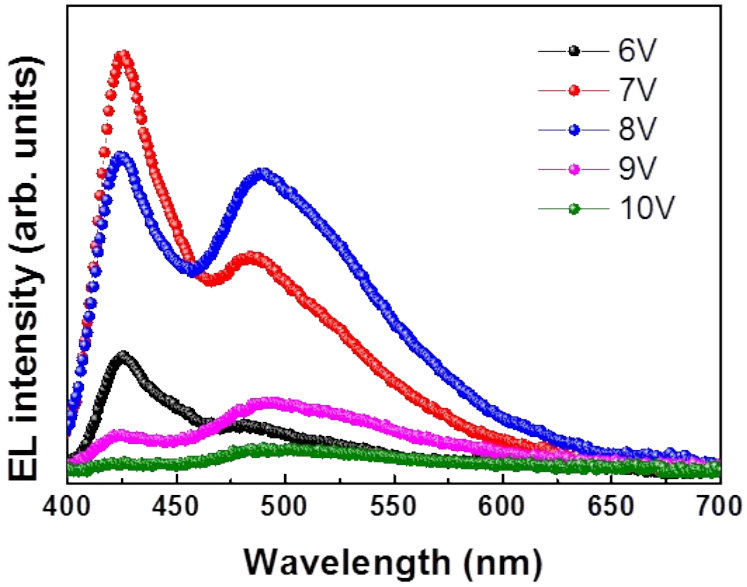

Figure S21. Electroluminescence spectra for the ZnO-C_{60} LEDs.

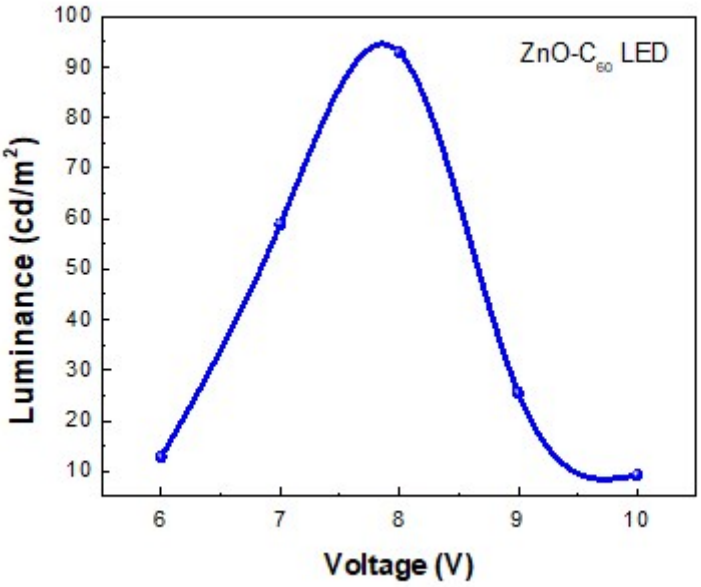

Figure S22. Luminance–voltage characteristics of the ZnO-C_{60} LEDs with applied voltages from 6 to 10 V.

C_{70}	HOMO [-5.92 eV]	LUMO [-3.24 eV]	LUMO+1 [-3.24 eV]	LUMO+2 [-3.15 eV]
s-orbital (%)	4.7	5.0	5.0	7.1
p-orbital (%)	95.0	94.6	94.6	92.6

Table S1. Table of Orbital Contributions related C_{70}.

Epoxy-C_{70}	HOMO [-5.97 eV]	LUMO [-3.29 eV]	LUMO+1 [-3.25 eV]	LUMO+2 [-3.21 eV]
s-orbital (%)	4.8	5.3	5.4	7.2
p-orbital (%)	94.9	94.3	94.2	92.5

Table S2. Table of Orbital Contributions related epoxy-C_{70}

Hydroxy-C_{70}	HOMO-1 (β) [-5.89 eV]	HOMO (α) [-5.18 eV]	LUMO (β) [-3.99 eV]	LUMO+1 (α) [-3.25 eV]	LUMO+2 (α) [-3.21 eV]
s-orbital (%)	4.8	7.2	8.1	4.9	6.3
p-orbital (%)	94.9	92.4	91.4	94.7	93.3
Hydroxy-C_{70}	LUMO+3 (β) [-3.19 eV]	LUMO+4 (β) [-3.13 eV]	LUMO+5 (α) [-2.80 eV]	LUMO+6 (β) [-2.72 eV]	
s-orbital (%)	5.9	5.9	5.8	5.6	
p-orbital (%)	93.8	93.8	93.8	93.9	

Table S3. Table of Orbital Contributions related hydroxy-C_{70}

Carboxy-C_{70}	HOMO-1 (β) [-5.91 eV]	HOMO (α) [-5.45 eV]	LUMO (β) [-4.13 eV]	LUMO+1 (α) [-3.28 eV]	LUMO+2 (β) [-3.21 eV]
s-orbital (%)	3.9	5.8	7.4	6.5	6.0
p-orbital (%)	95.7	93.7	92.2	93.1	93.6
Carboxy-C_{70}	LUMO+3 (α) [-3.17 eV]	LUMO+4 (β) [-3.08 eV]	LUMO+5 (α) [-2.92 eV]	LUMO+6 (β) [-2.81 eV]	
s-orbital (%)	7.0	7.5	5.8	6.4	
p-orbital (%)	92.7	92.1	93.8	93.2	

Table S4. Table of Orbital Contributions related carboxy-C_{70}

λ (nm)	f_1 (%)	τ_1 (ns)	f_2 (%)	τ_2 (ns)	τ_{avg} (ns)	χ^2
375	1.79	0.3423	98.21	0.014013	0.0199	1.161
385	3.19	1.530	96.81	0.018430	0.067	1.160
415	92.77	1.6846	7.23	0.10822	1.5706	1.360
460	74.92	1.9126	25.08	0.9302	1.6662	1.037

Table S5. PL lifetimes of ZnO-C_{60}.

λ (nm)	f_1 (%)	τ_1 (ns)	f_2 (%)	τ_2 (ns)	τ_{avg} (ns)	χ^2
375	1.52	0.748	98.48	0.024625	0.0356	1.299
385	4.04	1.780	95.96	0.022816	0.0940	1.515
415	90.34	1.6640	9.66	0.05693	1.5086	1.175
460	88.19	1.7975	11.81	0.6228	1.6587	1.034

Table S6. PL lifetimes of ZnO-C_{70}.

ZnO-C_{70}	x	y
4 V	0.2008	0.1725
5 V	0.1939	0.1666
6 V	0.1921	0.1799
7 V	0.1983	0.2482
8 V	0.2332	0.3272

Table S7. Table of CIE color coordinates of ZnO-C_{70} LEDs.

ZnO-C_{60}	x	y
6 V	0.2036	0.1795
7 V	0.1902	0.2079
8 V	0.2091	0.2883
9 V	0.2481	0.3634
10 V	0.2737	0.3889

Table S8. Table of CIE color coordinates of ZnO-C_{60} LEDs.